

Methods

To correlate fossil levels to the Geomagnetic Polarity Time Scale (GPTS), eight sections (Table A1) were measured in four areas of the Valley of Lakes (see Badamgarav et al. (1975) and Höck et al. (1999) for detailed descriptions of lithostratigraphy and sedimentology of the Hsanda Gol and related formations). Section EHG at Menkhen Teg spans the upper Elegen Formation and continues into the lower member of the Hsanda Gol Formation. Two sections were measured at Taatsin Gol, TGB and TGAB (directly corresponding to TGR-B and TGR-AB of Höck et al., (1999)). TGB spans the upper 15 m of the Elegen Formation and the Tatal member of Hsanda Gol Formation. The section is capped by 10 m of basalt, which can be traced to the base of section TGAB. TGAB is found only 50 m from TGB and includes the first 9 m of the Shand member of the Hsanda Gol Formation and is capped by an unconformable Loh Formation. The basalt was sampled for paleomagnetic analysis and was previously dated at 31.5 Ma (Höck et al., 1999)

Two sections were measured at Tatal Gol, Bryant's Hill and North Ridge. Bryant's Hill section is entirely within the Hsanda Gol Formation and includes a dated basalt (Höck et al., 1999) that is situated approximately 10 m from the base of the section. The section continues for nearly 20 m above the basalt. The base of North Ridge section is located just above the same basalt level as Bryant's Hill, although several interpretations of the correlation of these two sections are discussed below. Two sections were measured at Loh, LOH and ULP. The Loh section begins near the base of the

Hsanda Gol Formation and continues into the upper reaches of the Shand member. No basalt is exposed within this section. ULP is entirely within the Shand member of the Hsanda Gol Formation, and is found on the northeastern end of a prominent ridge of exposed Hsanda Gol Formation along the west side of the Loh drainage. The LOH section was measured on the southwestern end of this ridge. The two sections are correlated based on the occurrence of a white sandy layer that can be traced along the entire ridge. Section BO is across the Loh drainage from LOH and ULP and consists of several meters of sediments near the Hsanda Gol/Elegen contact.

Sediments from the Elegen and Hsanda Gol formations were collected from all measured sections in four different areas; radioisotopically dated basalt was found within the sections of two areas (Taatsin Gol and Tatal Gol). Oriented sediment samples for paleomagnetic study were collected in 1995 and 1997 (referred to as set A [$n = 55$], including Bryant's Hill, North Ridge, and LOH) and again in 2004 and 2006 (referred to as set B [$n = 45$], including Menkhen Teg, Taatsin Gol A and B, ULP, and BO). Field samples from 250 – 2,000 cm³ were collected in 1 m to 1.8 m stratigraphic increments, although deviations from these increments occurred due to lithological considerations. All samples were cut into smaller specimens (~ 11 cm³); two specimens for each sample for set A and three specimens from each sample from set B were prepared and demagnetized.

Remanence measurements of specimens from set A were made with a 2G Model 760 three-axis cryogenic magnetometer in a shielded room, which reduced the ambient field to $< 300\mu\text{T}$ at the Paleomagnetic Laboratory at Lamont-Doherty Earth Observatory (Columbia University). The natural remnant magnetization (NRM) was measured for

each specimen followed by a 14 step thermal demagnetization sequence: 200°, 300°, 400°, 500°, 525°, 550°, 575°, 600°, 625°, 650°, 660°, 670°, 680°, and 685° C. Between each demagnetization, the magnetic remanence as well as the susceptibility were measured. Remanence measurements of specimens from set B were made with a 2-G 755 cryogenic magnetometer in a magnetically shielded room (residual field < 2nT) at the Berkeley Geochronology Center. After measuring the NRM, specimens were demagnetized using both alternating field (AF) and thermal techniques; magnetic remanence was measured after each thermal step of demagnetization and before and after all AF demagnetization steps. AF was applied at 3, 6, 9, 12, and 15 mT to erase viscous remnant magnetization. Specimens were then thermally demagnetized beginning at 90°C and continuing to 625°C. All specimens were demagnetized (including AF and thermal) over 12 – 19 steps.

In general, each specimen began with a remanence that consisted of a low temperature/low coercivity component (aligned with the modern field direction) and a high temperature/high coercivity component (that was either of normal or reverse polarity) that was considered the Characteristic Remanent Magnetization (ChRM). Although it is difficult to distinguish the expected paleopole for the early Oligocene of this area (Hankard, et al., 2007) from the modern field due to their similar position, most normal samples did show two distinct normal components. Table A2 summarizes reverse and normal pole directs for each stratigraphic section. The low temperature component was typically removed by AF treatment (for set B) and heating to 200°C (AI Fig. 7, A). In some specimens, however, this component persisted into higher temperatures reaching 500°C and overlapped with a ChRM (see discussion below). Samples in which the

modern component was easily removed, revealing a high temperature component, and then showed decay to the origin in orthogonal projection, are considered Class A (n = 55). Some samples, however, exhibited a demagnetization pattern that suggested a broad overlap of the low and high temperature components. These samples showed strong great circle trends in stereo projection; long, dispersed trends in specimens with a reversed high component, and short trends in specimens with a normal high temperature component. Samples in which all specimens exhibit this broad overlap are considered Class C (n = 36), and samples that consist of specimens of both types are considered class B (n = 9).

Directions of ChRM for specimens that exhibited clear separation of ChRM from a low temperature component were calculated using least squares analysis as described by Kirschvink (1980). AI Fig. 7 shows both reversed and normal samples in orthogonal projection. Directions of ChRM specimens in which a strong trend within stereographic projection occurred, but the ChRM did not decay toward the origin in orthogonal projection, were calculated by determining a mean direction (in stereographic direction) of representative thermal steps ((Fisher, 1953); Supp. Fig. 7, F). In one sample, a strong great circle trend was observed between secondary and ChRM components, but no series of steps represented a specific direction at higher temperatures. In these specimens, the end of streak method (Scott, et al., 2007) was used and a terminal step along the great circle trend was taken as the direction of the ChRM. All statistical analysis on the demagnetization data was conducted using PaleoMac (Cogné, 2003)

Polarity could be determined for all samples presented here, but because samples that exhibited overlapping components show a mixture of multiple components at high temperatures, the high temperature component is not specifically an ancient field

direction. For this reason, Virtual Geomagnetic Pole (VGP) latitudes were not used. Instead, specimen and sample (mean for samples with multiple specimens) paleomagnetic directions were calculated as the angular difference (Δ) between the specimen (D_a, I_a) direction and the expected normal direction ($D_b = 358.2^\circ, I_b = 65.5^\circ$, from Hankard et al., (2007)), using the formula: $\Delta = \cos^{-1}(\cos I_A \cos D_A \cos I_B \cos D_B + \cos I_A \sin D_A \cos I_B \sin D_B + \sin I_A \sin I_B)$ from Butler (1992). In sample set A the characteristic specimen was typically used to determine direction rather than specimen means.

Results continued.

The placement of the upper fauna is more difficult as it is clear that a faunal hiatus occurs between the lower and upper faunas. The lowest stratigraphic positions of Tabenbulakian fossils within sections that can be related to those presented here occur at TGB and LOH, where Höck et al. (1999) show that Tabenbulakian fossils first appear ~10 m above the basalt (their TGL-A). TGL-A can be easily correlated to TGB via the basalt and due to the fact that the two areas were once stratigraphically continuous, but are now separated by erosion of the Taatsin Gol drainage. Based on the stratigraphic range of C12n within TGAB and the distribution of fossils at TGL-A, it is likely that the stratigraphically lowest Tabenbulakian fossils occur at the base of C11r. The upper age of the Tabenbulakan (and upper fauna of the Hsanda Gol Formation) is unclear due to the unconformity of the Hsanda Gol/Loh Formations.

Figure AI 8 shows the upper Elegen/lower Hsanda Gol sequence at TGB with associated stereographic summaries of paleomagnetic specimens. Important to note is the presence of a cryptochron (Cande and Kent, 1992) within the C13n ($\approx 33.3 - 33.7$ Ma) at

the base of the Hsanda Gol Formation. One TGB sample produced two specimens of reversed and one of normal polarity. The specimens of reversed polarity were cut from the same level within the sample, but the specimen of normal polarity was cut from a different level. To clarify the presence of two different polarities within the same sample, four new specimens were prepared from the original sample; two from the initially recognized reversed layer and two from the normal layer. All four new specimens were demagnetized using the same methods and showed the same polarities as previous specimens from the same levels within the sample. Because the sample itself is bounded above and below by normal polarity samples, the sequence overall is still correlated to magnetozone C13n. However, as a small reversed layer is observed within an otherwise normal sample a minor cryptochron is inferred in magnetozone C13n.

The three highest samples in C12r at TGB are likely overprinted by the overlying basalt. Although these samples show a strongly reversed ChRM, their increased intensity relative to other sediments within this section and lack of a low coercivity component suggest that they retain a magnetization derived due to baking as the overlying basalt was deposited. The lowest sample from this sequence is found just 2.3 m below the 10 m thick basalt layer and all of the samples show some degree of discoloration believed to be from a baking event. Because the basalt and the three samples below it are reversed, it is likely that the entire sequence represents C12r. The polarities of the overprinted samples are marked as questionable in figure 5 (denoted by question marks) to show that the magnetization is likely derived from the basalt, and not a ChRM derived during initial lithification of sediments.

Table DR1. Longitude and latitude coordinates for sections referenced in text.

Sections	Latitude	Longitude
BO	45° 14' 55"	101° 48' 55"
ULP	45° 16' 31"	101° 46' 34"
LOH	45° 16' 13"	101° 45' 54"
North Ridge	45° 18' 05"	101° 38' 31"
Bryant's Hill	45° 17' 52"	101° 37' 47"
TGAB	45° 24' 49"	101° 15' 25"
TGB	45° 24' 53"	101° 15' 44"
EHG	45° 24' 31"	101° 04' 03"

Table DR2. Fisher mean (1953) averages for normal and reversed specimens in each section

Sections	Specimen polarities	Direction means		n	k	α_{95}
		Inc.	Dec.			
TGB	N	355.7	57.9	11	53.4	7.1
	R	174.8	-47.8	36	9.4	8.2
TGAB	N	348.7	65.4	19	24.7	6.9
	R	168.5	-50.2	2	1344.8	6.8
ULP	N	357.0	64.0	30	22.2	5.7
EHG	N	352.7	63.6	7	2.9	43.2
	R	187.2	-33.6	9	4.3	28.3
Tatal ^a	N	346.9	61.0	11	5.5	21.4
	R	204.4	-56.2	13	6.6	17.5
Loh	N	341.6	54	7	7.9	19.8
	R	173.8	-60.6	25	9.7	9.8
BO	N	4.3	65.3	5	133.1	6.7
^a note: that Tatal refers to a combined Bryant's Hill and North Ridge sections						

REFERENCES CITED

- Badamgarav, D., Dashzeveg, D., Devyatkin, E. V., Zhegallo, V. I., and Liskun, I. G., 1975, Stratigrafiya Paleogena I Neogena Dolina Ozer (K vorposu o vydelenii sratotipicheskogo rayona dlya Paleogena I Neogena Tsentral'noy Azii), in Kramarenko, H. N., ed., Trudy - Sovmestnaya Sovetsko-Mongol'skaya Paleontologicheskaya Ekspeditsiya, p. 250–268.
- Butler, R. F., 1992, Paleomagnetism: Magnetic Domains to Geologic Terranes: Blackwell Scientific Publications: Boston, pp. 319.
- Cogné, J. P., 2003, PaleoMac: A Macintosh™ application for treating paleomagnetic data and making plate reconstructions: Geochemistry, Geophysics, and Geosystems, v.

4, p. 1007.

Fisher, R., 1953, Dispersion on a sphere: Proceedings of the Royal Society of London, Series A, No. 217, p. 295–305.

Hankard, F., Cogné, J. -P., Kravchinsky, V. A., Carporzen, L., Bayasgalan, A., and Lkhagvadorj, P., 2007, New Tertiary paleomagnetic poles from Mongolia and Siberia at 40, 30, 20, and 13 Ma: Clues on the inclination shallowing problem in central Asia, *Journal of Geophysical Research*, v. 112, B02101.

Höck, V., Daxner-Höck, G., Schmid, H. P., Badamagarav, D., Frank, W., Furtmüller, G., Montag, O., Barsbold, R., Khand, Y., Sodov, J., 1999, Oligocene–Miocene sediments, fossils and basalts from the valley of the lakes (Central Mongolia): An Integrates study: *Mitteilungen der Österreichischen Geologischen Gesellschaft*, v. 90, p. 83–125.

Kirschvink, J. L., 1980, The least-square line and plane and the analysis of paleomagnetic data: *Geophysical Journal International*, v. 62, p. 699–718.

Scott, G. R., Gibert, L., Gibert, J., 2007, Magnetostratigraphy for the Orce region (Baza Basin), SE Spain: New chronologies for Early Pleistocene faunas and hominid occupation sites: *Quaternary Sciences Reviews*, v. 26, p. 415–435.

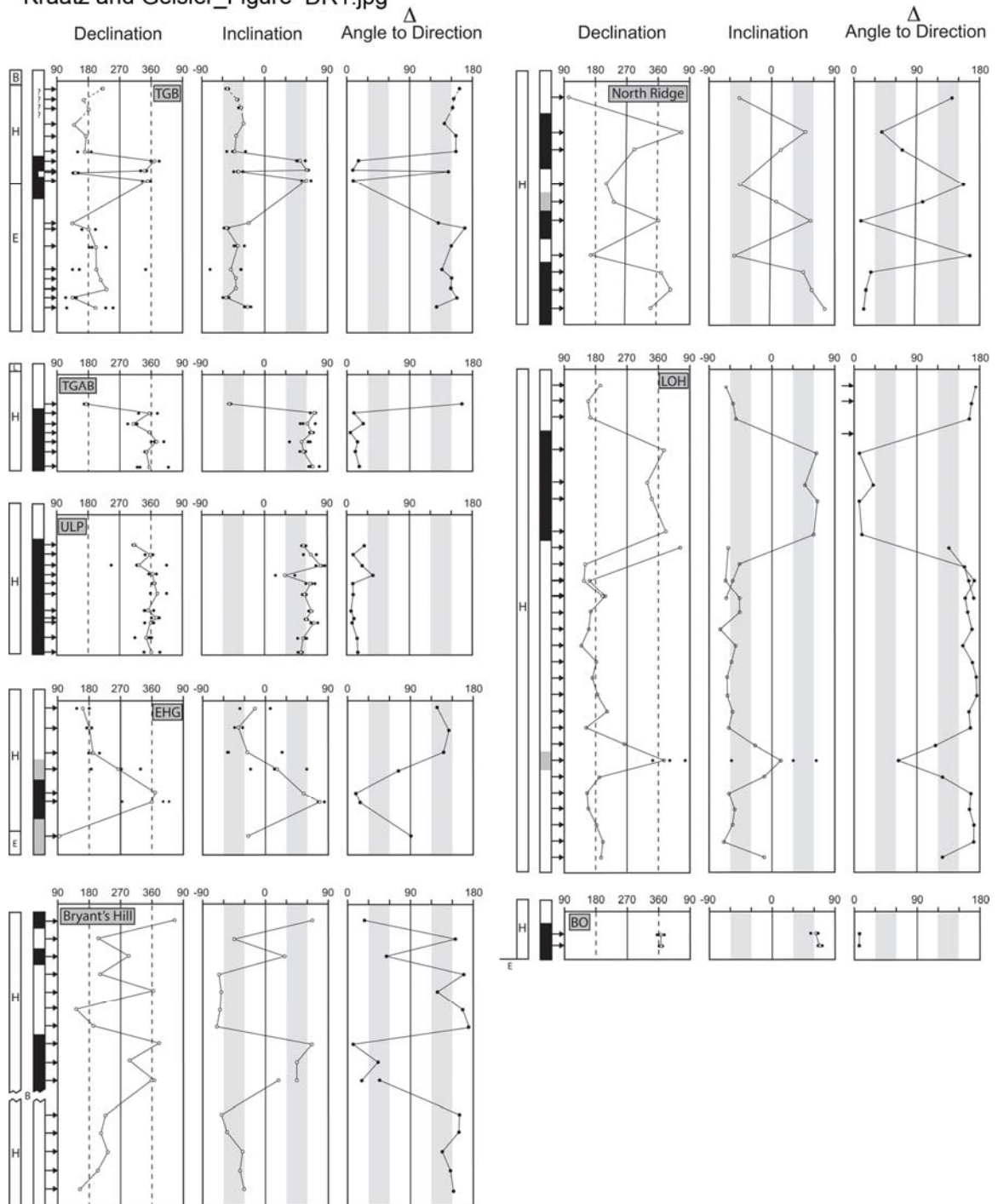


Figure DR1. Declination, Inclination, and Angle to Direction data for all samples in study. For samples with multiple specimens, sample means are marked by unfilled circle, and a solid circle marks individual specimens. On stratigraphic columns to the left of each section, B denotes basalt, L denotes Loh formation, H denotes Hsanda Gol formation, and E denotes Elegen formation. See supplemental text for a discussion of the Angle to Direction method.

Kraatz and Geisler_Figure DR2.jpg

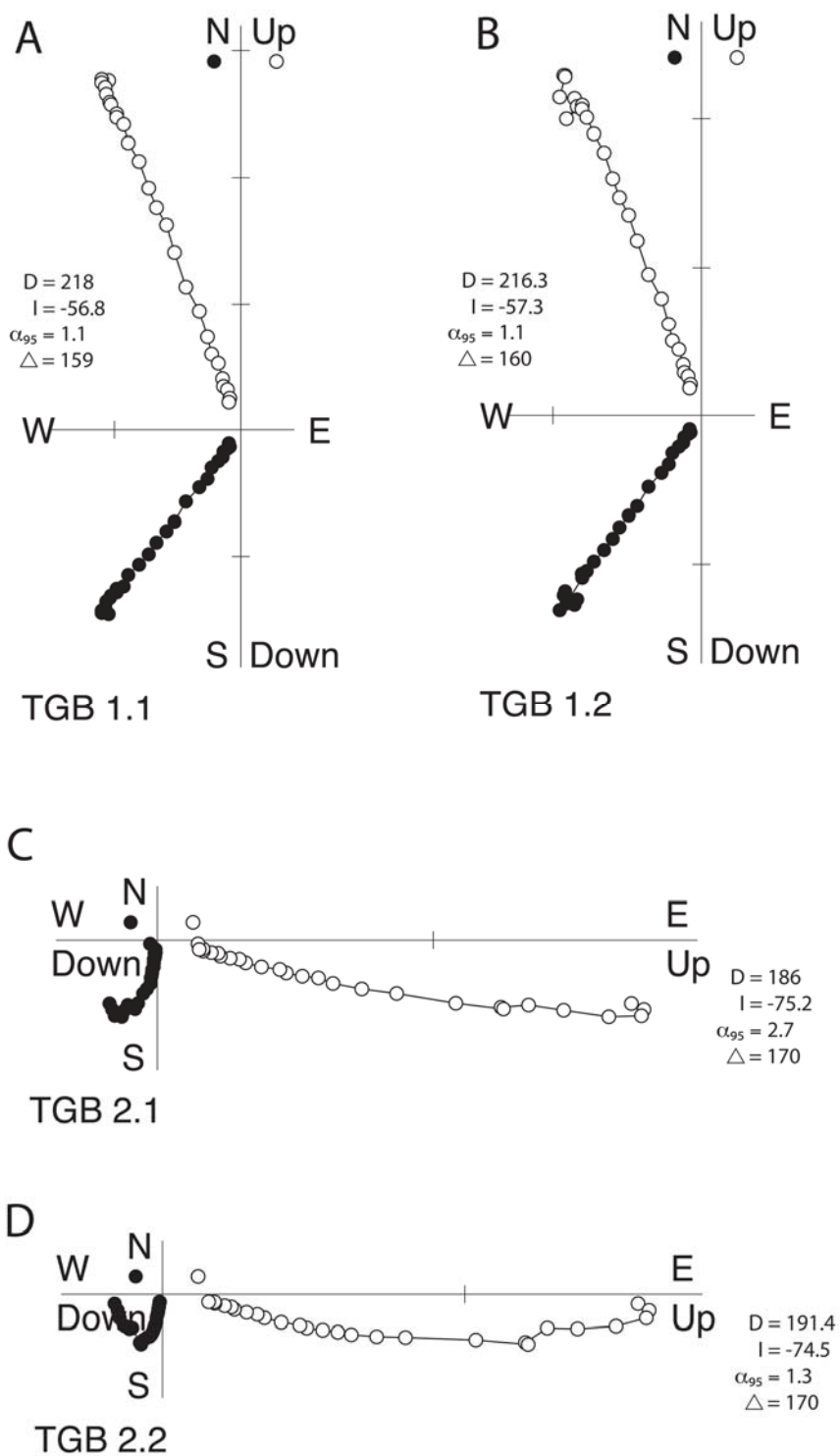


Figure DR2. Orthogonal projection of 4 specimens (two samples) taken from the basalt at TGB and TGAB. One sample (TGB.1, A and B of this figure) is from the top of the ~ 10 m basalt, the other (TGB.2, C and D of this figure) is from the bottom of the basalt.

Figure 5

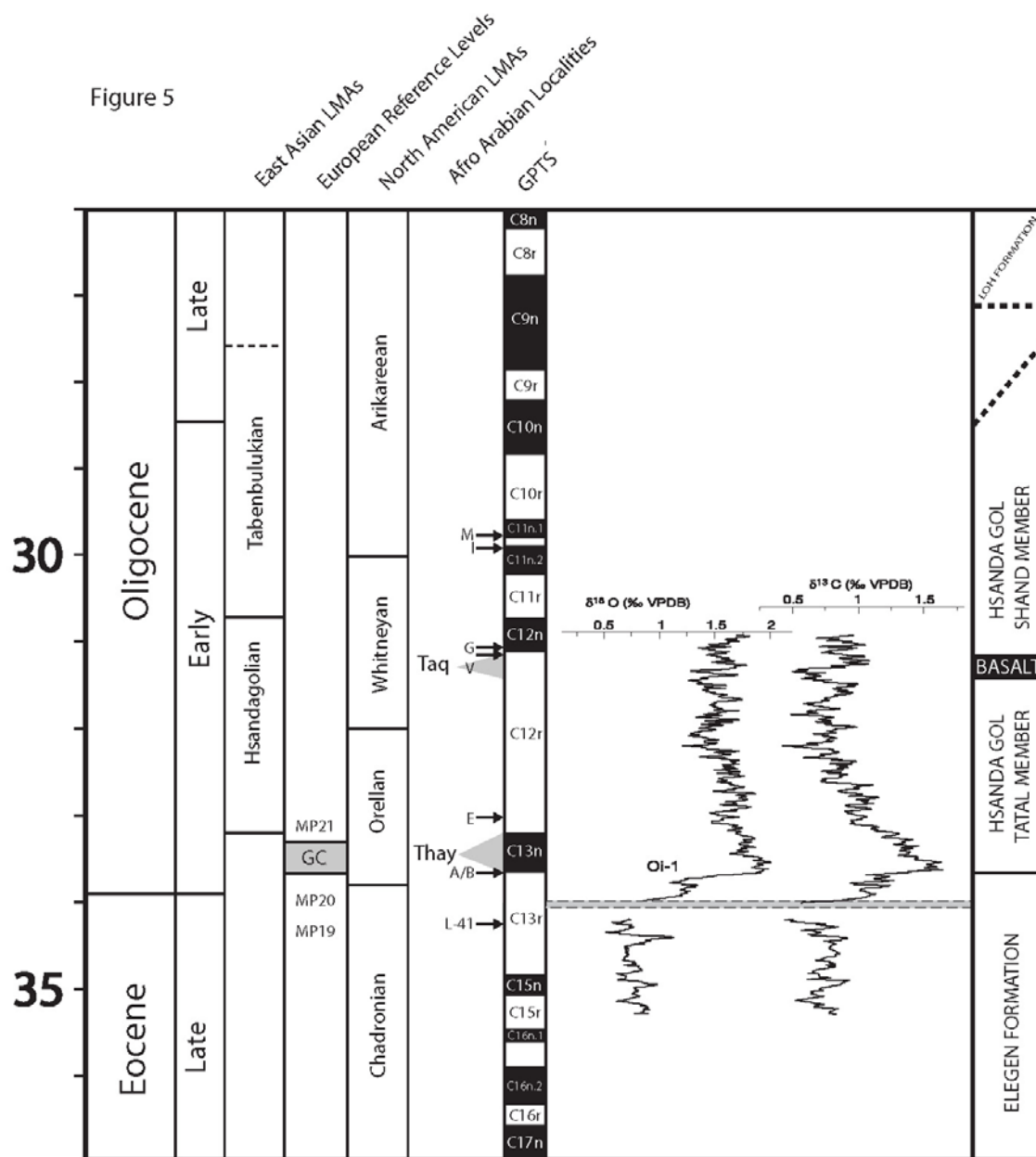


Figure DR3. Correlation of Hsanda Gol Formation to East Asian Land Mammal Ages as well as those from Europe, North America, and Afro-Arabia. Time scale and GPTS are taken from Gradstein et al., (Gradstein, et al., 2004). Placement of European reference levels are based on Hooker et al. (Hooker, et al., 2004). North American Land Mammal Ages and Afro-Arabian localities are taken from Woodburne (2004) and Seiffert (2006) respectively. The $\delta^{18}\text{O}$ and $\delta^{13}\text{C}$ curves are taken from Coxall et al. (2005) and mark major climatic excursions as well as the onset of Antarctic glaciation (Oi-1). The schematic of the Hsanda Gol Formation is not to scale.

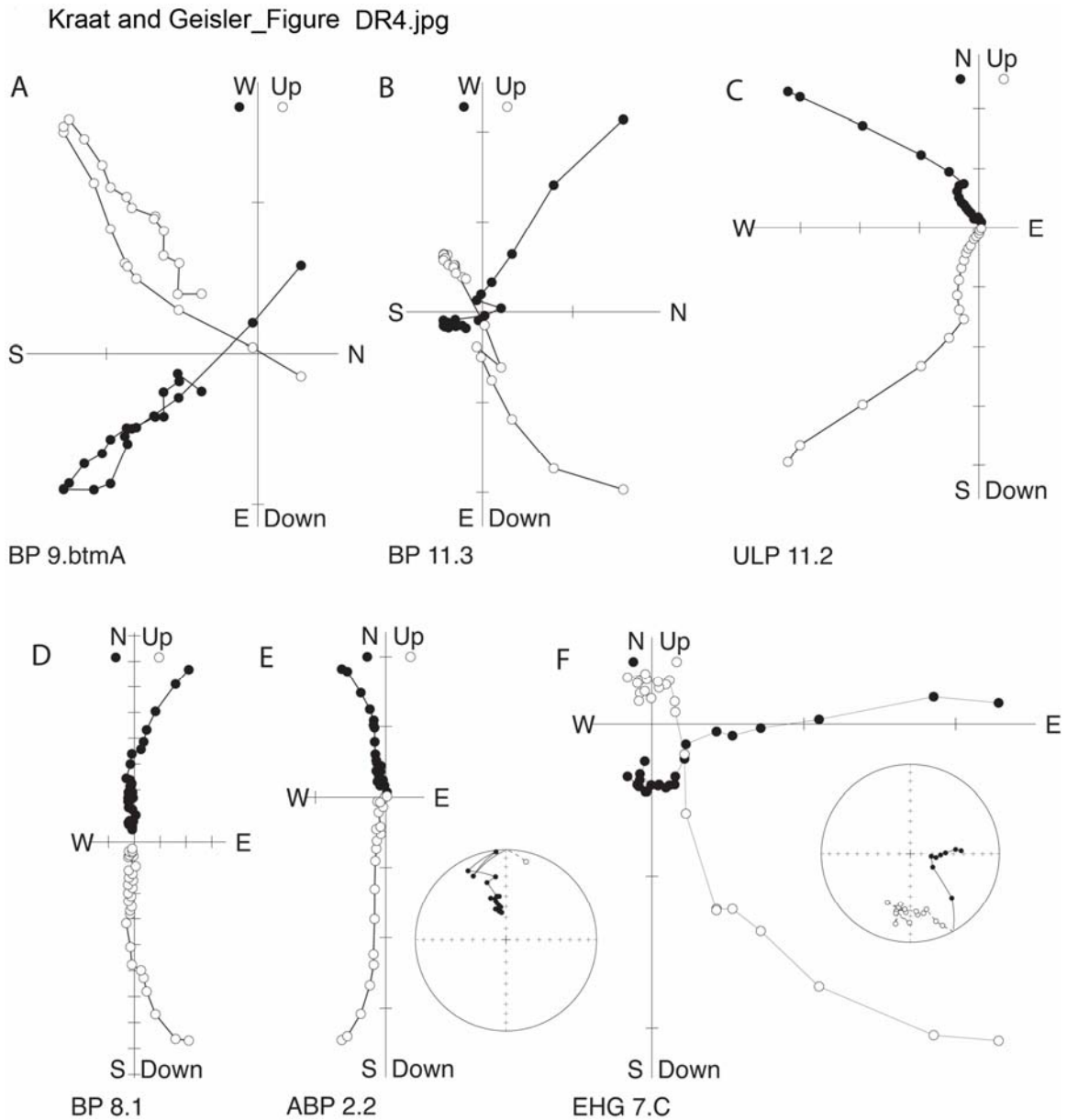


Figure DR4. Orthogonal projections of typical specimens, see supplemental text for discussion of what constitutes specimen types A, B, and C. A and B represent reversed specimens of type A. C and D represent normal polarity specimens of type A. F shows a sample (as discussed in text) in which a strong great circle trend during demagnetization is observed, but the specimen does not decay toward the origin (type C). Planes in stereographic projection represented by orthogonal axes are denoted in each graph.

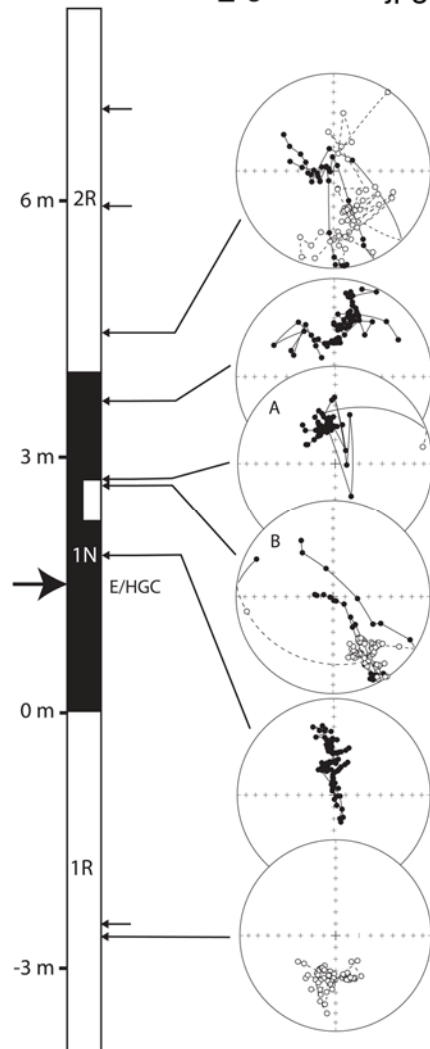


Figure DR5. A portion of section TGB that spans the Elegen/Hsanda Gol contact (denoted by arrow and E/HG in figure) and includes a normal polarity zone at the base of the Hsanda Gol Formation that is correlated to C13n of the GPTS. Arrows on right represent all levels from which paleomagnetic samples were taken. Stereographic projections are shown for six samples that illustrate the transition from reversed to normal and back to reversed polarities from stratigraphically low to high samples. Stereographic projections A and B also show two different specimens from the same sample that are of different polarity and have been interpreted to span a cryptochron (see text for discussion).